



New monoclinic compounds, $\text{Bi}_{3.24}\text{Ln}_2\text{W}_{0.76}\text{O}_{10.14}$, having a pseudo-orthohexagonal cell based on a pseudo-fcc subcell in the systems $\text{Bi}_2\text{O}_3\text{--Ln}_2\text{O}_3\text{--WO}_3$ ($\text{Ln} = \text{La, Pr, and Nd}$)

Akiteru Watanabe*

Advanced Materials Laboratory, National Institute for Materials Science, 1-1 Namiki, Tsukuba-shi, Ibaraki 305-0044, Japan

Received 19 March 2002; received in revised form 24 June 2002; accepted 20 August 2002

Abstract

New compounds, $\text{Bi}_{3.24}\text{Ln}_2\text{W}_{0.76}\text{O}_{10.14}$, have been found in the systems $\text{Bi}_2\text{O}_3\text{--Ln}_2\text{O}_3\text{--WO}_3$ ($\text{Ln} = \text{La, Pr, and Nd}$). They crystallize ostensibly in the orthorhombic (or orthohexagonal) symmetry, e.g. with $a = 6.9694(1) \text{ \AA}$, $b = 4.0242(1) \text{ \AA}$, $c = 9.3335(1) \text{ \AA}$, and $Z = 1$ for $\text{Ln} = \text{La}$. At the same time, the lattice forms a superstructure based on a pseudo-fcc subcell with $a' \approx 5.6 \text{ \AA}$, where the transformation matrix is $(1/2, 1/2, -1)/(-1/2, 1/2, 0)/(1, 1, 1)$. However, the cation configuration has proved that the true symmetry is monoclinic ($C2/m$) with $\beta \approx 90^\circ$. All new compounds undergo two reversible polymorphic transitions at about 980°C and at $1097\text{--}1210^\circ\text{C}$ depending on Ln . Their electrical conductivity exhibited lower values (about $10^{-4} \text{ S cm}^{-1}$ at 500°C) despite the pseudo-fcc subcell in relation to the $\delta\text{-Bi}_2\text{O}_3$ type which is the well-known good oxide-ion conductor.

© 2002 Elsevier Science (USA). All rights reserved.

Keywords: New compounds $\text{Bi}_{3.24}\text{Ln}_2\text{W}_{0.76}\text{O}_{10.14}$ ($\text{Ln} = \text{La, Pr, and Nd}$); Orthohexagonal symmetry; Superstructure; Pseudo-fcc subcell; Monoclinic symmetry; Two reversible polymorphic transitions

1. Introduction

In the ternary systems $\text{Bi}_2\text{O}_3\text{--Ln}_2\text{O}_3\text{--WO}_3$ ($\text{Ln} = \text{La--Lu, and Y}$), the subsolidus phase equilibrium study found a series of monoclinic layered $\text{Bi}_{2-x}\text{Ln}_x\text{WO}_6$ solid solutions within limited compositional ranges [1,2]. Although these solid solutions can be regarded as formed by the partial substitution of Ln for Bi in orthorhombic Bi_2WO_6 [3,4] which is the simplest member of the Aurivillius family [5], the substitution led to not only the symmetrical change from orthorhombic to monoclinic but also the coordination number of tungsten from the corner-shared WO_6 octahedron [3] to the isolated WO_4 tetrahedron [1,6]. The structural change was explained qualitatively by the interaction between Bi^{3+} and Ln^{3+} [2] and by the $6s^2$ lone pair repulsion [7]. Thus, since these systems are very attractive from a crystallochemical viewpoint, the subsequent phase research study has recently been done.

As a result, new compounds $\text{Bi}_{3.24}\text{Ln}_2\text{W}_{0.76}\text{O}_{10.14}$ have been identified only in $\text{Ln} = \text{La, Pr, and Nd}$ in contrast to the above-mentioned solid solutions with all Ln 's. These new compounds form a superstructure based on a pseudo-fcc subcell. The superstructure can be considered to have an orthohexagonal lattice; nevertheless, the configuration of cations indicates that the true symmetry is monoclinic with $\beta \approx 90^\circ$.

2. Experimental procedures

The starting materials were 99.9% pure Bi_2O_3 , Ln_2O_3 ($\text{Ln} = \text{La, Nd, Sm, Eu, Gd, Dy, Ho, Er, Tm, Yb, Lu, and Y}$), Pr_6O_{11} , Tb_4O_7 , and WO_3 . The lanthanoid oxides were pre-fired for dehydration at 600°C in air before use. The desired proportions of $(\text{Bi}_2\text{O}_3)_x(\text{Ln}_2\text{O}_3)_y(\text{WO}_3)_z$, where $x + y + z = 1$ and $x > 0.4$, were accurately weighed and thoroughly hand-mixed in an agate mortar and a pestle. The mixture was transferred into a covered platinum crucible, heated at 1000°C for 20 h or more, and quenched by an air stream to room

*Fax: +81-298-52-7449.

E-mail address: watanabe.akiteru@nims.go.jp (A. Watanabe).

temperature. The same heat treatment was repeated after intermediate grindings to complete the reaction. Every time the samples were quenched, they were examined by X-ray powder diffraction (XRPD) method using $\text{CuK}\alpha$ radiation and a diffracted-beam monochromator.

To check the crystal system and preliminary lattice parameters of new phases, Visser's indexing program [8] was applied to the observed XRPD data measured with a continuous scanning method at a scanning rate of $0.4^\circ (2\theta) \text{ min}^{-1}$ over the angular range $5\text{--}135^\circ (2\theta)$. The 2θ values were corrected using the external standard of a Si powder. The precise lattice parameters were calculated by the least-squares method [9]. In addition, a proposed structural model was examined by the Rietveld method using the RIETAN refinement program [10] on the data scanned by steps of $0.02^\circ (2\theta)$ over $9\text{--}134^\circ$ with a counting time of 15 s per step.

The density of the powder sample was measured using a gas pycnometer (Micromeritics Accupyc 1330). The sample weight was about 20 g.

The thermal behavior was checked by differential thermal analysis (DTA) with an apparatus of Rigaku TG-8120. About 50 mg of the powder sample put in a platinum sample holder underwent heating-cooling cycles in air to a maximum temperature of 1300°C in a subsolidus region. The heating-cooling rate was $10^\circ\text{C min}^{-1}$. The reference material was $\alpha\text{-Al}_2\text{O}_3$, and the temperature accuracy was $\pm 3^\circ\text{C}$.

Electrical conductivity was measured in air by means of the impedance spectroscopy method on pellets smeared with gold paste as electrodes. To fabricate the pellets, the powder sample was prepressed uniaxially (10 mm in diameter and about 2 mm in thickness), then pressed isostatically at 200 MPa, and sintered at 1050°C for 10 h. The pellets were studied using a Solartron SI-1260 impedance analyzer in the frequency range 1 Hz–1 MHz at every 20°C interval between 210°C and 810°C through a heating-cooling cycle. The sample pellets were equilibrated at constant temperature for 20 min before each measurement.

3. Results and discussion

By changing x and y in $(\text{Bi}_2\text{O}_3)_x(\text{Ln}_2\text{O}_3)_y(\text{WO}_3)_{1-x-y}$, we could find new compounds $\text{Bi}_{3.24}\text{Ln}_2\text{W}_{0.76}\text{O}_{10.14}$ ($x = 0.4793$ and $y = 0.2959$) only in $\text{Ln} = \text{La}$, Pr, and Nd. Fig. 1 shows the XRPD pattern for $\text{Ln} = \text{La}$. Since the same patterns were obtained in both Pr and Nd, all three compounds seem to be isomorphous. Seeing that these three Ln^{3+} cations have relatively large effective ionic radii [11] ($r_{\text{La}} = 1.160 \text{ \AA}$, $r_{\text{Pr}} = 1.126 \text{ \AA}$, and $r_{\text{Nd}} = 1.109 \text{ \AA}$ for eight-fold coordination), an isomorphous compound may be prepared in $\text{Ln} = \text{Ce}^{3+}$ ($r_{\text{Ce}} = 1.143 \text{ \AA}$). Nevertheless, a preliminary synthesis

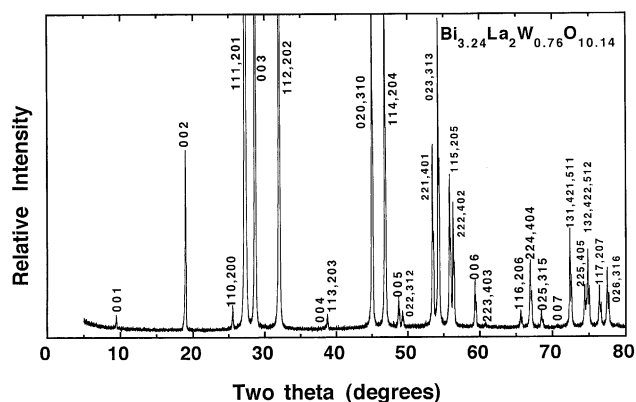


Fig. 1. Room-temperature XRPD pattern of $\text{Bi}_{3.24}\text{La}_2\text{W}_{0.76}\text{O}_{10.14}$ ($\lambda = \text{CuK}\alpha$). Miller indices based on the orthorhombic cell are indicated.

from $\text{Ce}(\text{NO}_3)_3$ as a starting material was completely unsuccessful. By contrast, in the cases of the other Ln 's, their XRPD patterns showed an fcc symmetry with a lattice constant of about 5.6 \AA ; these fcc phases appear to have a $\delta\text{-Bi}_2\text{O}_3$ -type structure [12].

The XRPD pattern of the stronger main reflections in Fig. 1 suggests that the new compounds may have a hexagonal lattice ($\mathbf{a}_H, \mathbf{b}_H, \mathbf{c}_H$) (or a rhombohedral one ($\mathbf{a}_{R1}, \mathbf{a}_{R2}, \mathbf{a}_{R3}$)) derived from an fcc lattice ($\mathbf{a}_{C1}, \mathbf{a}_{C2}, \mathbf{a}_{C3}$) as shown in Fig. 2. However, in Fig. 1, we can observe several weak reflections which imply the true unit cell is a supercell based on a pseudo-fcc subcell ($\mathbf{a}'_{C1}, \mathbf{a}'_{C2}, \mathbf{a}'_{C3}$) rather than the hexagonal cell. According to expectation, the indexing result of the computer program indicated that $\text{Bi}_{3.24}\text{La}_2\text{W}_{0.76}\text{O}_{10.14}$ crystallizes in the orthorhombic system, and the precise lattice parameters were calculated: $a = 6.9694(1) \text{ \AA}$, $b = 4.0242(1) \text{ \AA}$, $c = 9.3335(1) \text{ \AA}$, and $V = 261.780(8) \text{ \AA}^3$. The Miller indices based on these lattice constants are allocated to the reflections as shown in Fig. 1. The observable reflections are hkl with $h+k=2n$ and $00l$ all orders; these conditions designate a C-centered orthorhombic lattice and lead to the possible space groups $C222$, $Cmmm$, $Cmm2$, $Cm2m$, and $C2mm$. The axial relationships between the orthorhombic cell and the pseudo-fcc cell ($d \approx 5.6 \text{ \AA}$) are seen from Figs. 2 and 3a via the hexagonal (rhombohedral) cell. It is also evident from Fig. 3a that the orthorhombic cell has a C-centered lattice. This kind of orthorhombic cell is called the orthohexagonal cell [13]. In addition, these axial relationships yield the transformation matrix for the direct-lattice unit-cell vectors from the pseudo-fcc lattice (\mathbf{a}') to the orthorhombic one ($\mathbf{a}, \mathbf{b}, \mathbf{c}$): $(1/2, 1/2, -1)/(-1/2, 1/2, 0)/(1, 1, 1)$. Now that the measured density was 7.959 g cm^{-3} , it is obvious from this value and the cell volume that the orthorhombic cell contains one formula weight, $Z = 1$. On the one hand, the value of the determinant of the transformation, 1.5,

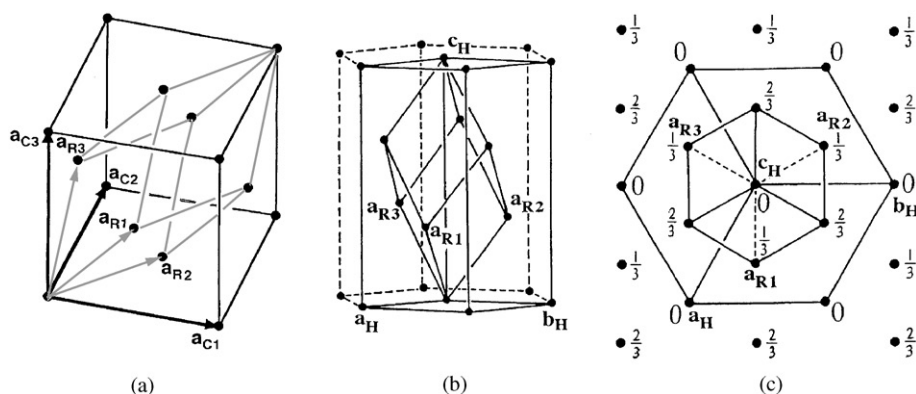


Fig. 2. Axial relationships between fcc and hexagonal cells through a rhombohedral cell: (a) the primitive rhombohedral cell (\mathbf{a}_{R1} , \mathbf{a}_{R2} , \mathbf{a}_{R3}) in the fcc cell (\mathbf{a}_{C1} , \mathbf{a}_{C2} , \mathbf{a}_{C3}), (b) the triple hexagonal cell (\mathbf{a}_H , \mathbf{b}_H , \mathbf{c}_H), in relation to the primitive rhombohedral cell, and (c) the projection of the three triple hexagonal cells and the primitive rhombohedral cell on the hexagonal (001) plane. The number on each lattice point is its fractional z coordinate.

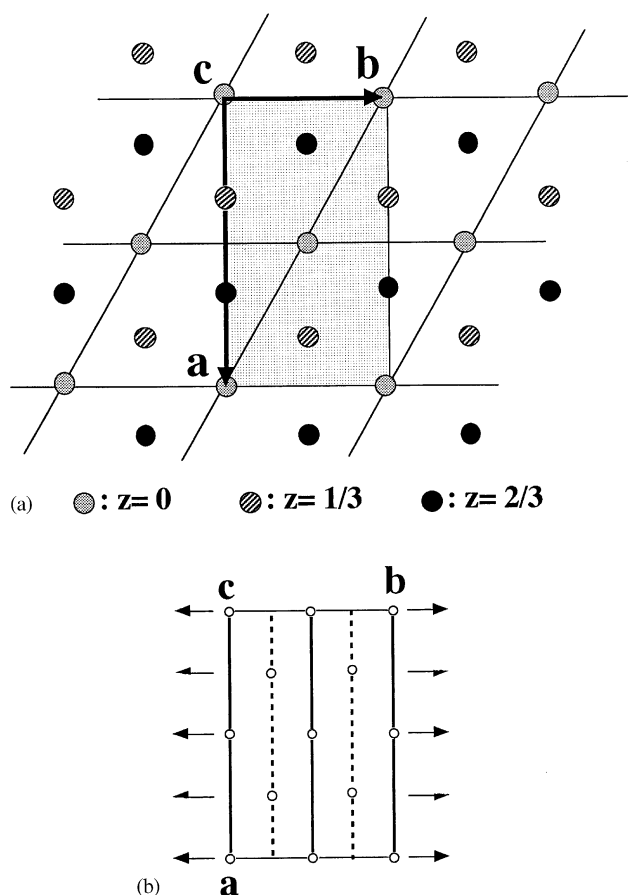


Fig. 3. Monoclinic configuration of cations: (a) the orthohexagonal cell (\mathbf{a} , \mathbf{b} , \mathbf{c}) and the cations projected on the (001) plane, and (b) the monoclinic space group $C2/m$ derived from the cation positions.

shows that the volume of the orthorhombic cell is 1.5 times the size of the pseudo-fcc subcell. Seeing that the fcc cell contains four lattice points, there exist $4 \times 1.5 = 6$ lattice points in the orthorhombic cell. This result agrees well with the number of cations included in the

orthorhombic cell, i.e., $Z = 1 \times (\text{Bi}_{3.24}\text{La}_2\text{W}_{0.76}\text{O}_{10.14})$. Therefore, the formation of the orthorhombic phase may be due to the ordering of Bi, Ln, and W cations.

From Fig. 3a, we can easily estimate the ideal coordinates for six cations: $0, 0, 0$; $1/2, 1/2, 0$; $1/3, 0, 1/3$; $5/6, 1/2, 1/3$; $2/3, 0, 2/3$; $1/6, 1/2, 2/3$. However, against expectation, any of the five possible space groups given above cannot explain these coordinates. Since this fact implies that the true symmetry is not orthorhombic, we checked the symmetry of the unit cell exhibited in Fig. 3a. The result indicates a monoclinic symmetry as shown in Fig. 3b. That is, the true space group is $C2/m$ [14] with $\beta \approx 90^\circ$. Thus, the monoclinic lattice parameters of $\text{Bi}_{3.24}\text{Ln}_2\text{W}_{0.76}\text{O}_{10.14}$ were recalculated, and the results are shown in Table 1 together with the pseudo-orthorhombic lattice parameters and the measured and calculated densities. For $\text{Bi}_{3.24}\text{La}_2\text{W}_{0.76}\text{O}_{10.14}$, Table 2 lists the Miller indices based on the monoclinic lattice, the observed and calculated d values, and relative intensities; at the same time, the fundamental reflections based on the pseudo-fcc subcell are juxtaposed in terms of $h'k'l'$.

To deduce an outline of the monoclinic structure, the atoms were assigned to the equipoints in $C2/m$ as follows. The two Ln atoms are put to the special positions $2a$. The other four cations, 3.24Bi and 0.76W atoms, can statistically occupy the special positions $4i$ where $x = 1/3$ and $z = 1/3$. All the O atom coordinates were estimated on the basis of the fluorite-type arrangement; furthermore, the O atoms can also statistically occupy three sets of the special positions $4i$: O(1) with $x = 1/3$ and $z = 1/12$, O(2) with $x = 1/6$ and $z = 5/12$, and O(3) with $x = 0$ and $z = 1/4$. Therefore, although the occupancy factors of the cations are 1, those of the O atoms are $10.14/(3 \times 4) = 0.845$. Fig. 4 shows the result of the best Rietveld refinement of $\text{Bi}_{3.24}\text{La}_2\text{W}_{0.76}\text{O}_{10.14}$ on the data listed in Table 3. The agreement of calculated and observed XRPD peaks gave

Table 1

Monoclinic and pseudo-orthohexagonal lattice parameters and measured (d_m) and calculated (d_c) densities of $\text{Bi}_{3.24}\text{Ln}_2\text{W}_{0.76}\text{O}_{10.14}$

<i>Ln</i>	<i>a</i> (Å)	<i>b</i> (Å)	<i>c</i> (Å)	β (deg)	<i>V</i> (Å ³)	d_m (g cm ⁻³)	d_c (g cm ⁻³)
La	6.9693(2)	4.0242(1)	9.3334(2)	89.996(3)	261.77(1)	7.959	7.972
	6.9694(1)	4.0242(1)	9.3335(1)		261.780(8)		
Pr	6.8802(3)	3.9729(1)	9.3231(3)	89.998(5)	254.85(1)	8.186	8.215
	6.8803(2)	3.9729(1)	9.3232(2)		254.856(9)		
Nd	6.8529(3)	3.9575(1)	9.3181(3)	89.994(5)	252.71(1)	8.308	8.328
	6.8532(2)	3.9575(1)	9.3183(2)		252.730(8)		

Table 2

X-ray powder diffraction data for $\text{Bi}_{3.24}\text{La}_2\text{W}_{0.76}\text{O}_{10.14}$

<i>h</i>	<i>k</i>	<i>l</i>	d_{calc} (Å)	d_{obs} (Å)	I_{obs}	<i>h' k' l'</i> ^a
0	0	1	9.333	9.320	1	
0	0	2	4.667	4.663	11	
1	1	0	3.485	3.482	2	
2	0	0	3.485			
1	1	1	3.2648			
1	1	-1	3.2648	3.2624	100	-111, 1-11
2	0	1	3.2646			
0	0	3	3.1111			
1	1	2	2.7923	2.7910	46	111
2	0	-2	2.7921			
0	0	4	2.3334	2.3334	1	
2	0	3	2.3208			
1	1	-3	2.3208	2.3203	1	
0	2	0	2.0121			
3	1	0	2.0119	2.0117	25	-220
1	1	4	1.9389			
2	0	4	1.9389	1.9385	23	20-2, 02-2
1	1	-4	1.9389			
0	0	5	1.8667	1.8667	2	
0	2	2	1.8477			
3	1	2	1.8476	1.8472	1	
3	1	-2	1.8475			
2	2	1	1.7130	1.7126	12	-311, 1-31
4	0	-1	1.7127			
0	2	3	1.6895	1.6895	19	11-3
3	1	3	1.6895			
3	1	-3	1.6894	1.6895	19	-131, 3-11
1	1	5	1.6455			
1	1	-5	1.6455	1.6454	9	13-1, 31-1
2	0	-5	1.6454			
2	2	-2	1.6324	1.6323	8	1-13, -113
4	0	2	1.6323			
0	0	6	1.5556	1.5554	3	311, 131
3	1	4	1.5238			
2	2	3	1.5203	1.5205	1	113
1	1	6	1.4205			
2	0	6	1.4205	1.4204	1	-222, 2-22
1	1	-6	1.4205			
2	2	4	1.3962	1.3960	4	22-2
4	0	-4	1.3960			
0	2	5	1.3685	1.3684	1	222
3	1	5	1.3685			
3	1	-5	1.3684			040, 400
						004

Table 2 (continued)

<i>h</i>	<i>k</i>	<i>l</i>	d_{calc} (Å)	d_{obs} (Å)	I_{obs}	<i>h' k' l'</i> ^a
0	0	7	1.3333	1.3328	1	
1	3	-1	1.3043			
4	2	-1	1.3042	1.3041	6	3-31, -331
5	1	1	1.3042			
2	2	-5	1.2738			
2	2	-5	1.2738	1.2738	3	1-33, 3-13
4	0	5	1.2737			
1	3	2	1.2677	1.2675	5	33-1
4	2	2	1.2676			
5	1	-2	1.2676			
2	0	7	1.2453	1.2452	3	-240, 420
1	1	-7	1.2453			
0	2	6	1.2307	1.2305	4	0-24, -204
3	1	6	1.2307			
3	1	-6	1.2306			
5	1	3	1.2129	1.2131	1	331
4	2	-3	1.2129			
0	0	8	1.1667	1.1664	1	133, 313
3	3	0	1.1617			
6	0	0	1.1616	1.1615	2	402, 042
1	3	-4	1.1471			
5	1	4	1.1470	1.1470	3	420, 240
4	2	-4	1.1470			
0	2	7	1.1115			
3	1	7	1.1115	1.1115	1	204, 024
3	1	-7	1.1114			
1	1	8	1.1063	1.1064	2	
2	0	-8	1.1063			
3	3	3	1.0883	1.0882	2	242, 422
3	3	-3	1.0883			
6	0	3	1.0882			
6	0	-3	1.0882	1.0882	2	224
1	3	5	1.0763			
4	2	5	1.0762	1.0761	2	-511, 1-51
5	1	-5	1.0761			
2	2	7	1.0589	1.0588	1	-333, 3-33
4	0	-7	1.0588			
0	0	9	1.0370	1.0370	1	33-3
0	2	8	1.0093			
3	1	-8	1.0092	1.0094	1	11-5
0	4	0	1.0061			
6	2	0	1.0060	1.0060	1	-151, 5-11

^a Miller indices based on the pseudo-fcc subcell.

$R_{\text{wp}} = 17.22\%$, $R_{\text{p}} = 12.06\%$, and $S = R_{\text{wp}}/R_{\text{exp}} = 3.78$. Thus, the actual positions of the cations are probably not far from the proposed ones, but the coordinates of the O atoms are hypothetical because of the far lower

atomic scattering factor than those of the cations. To determine the actual structure, especially the oxygen positions, a single-crystal X-ray diffraction analysis or a neutron diffraction analysis is needed.

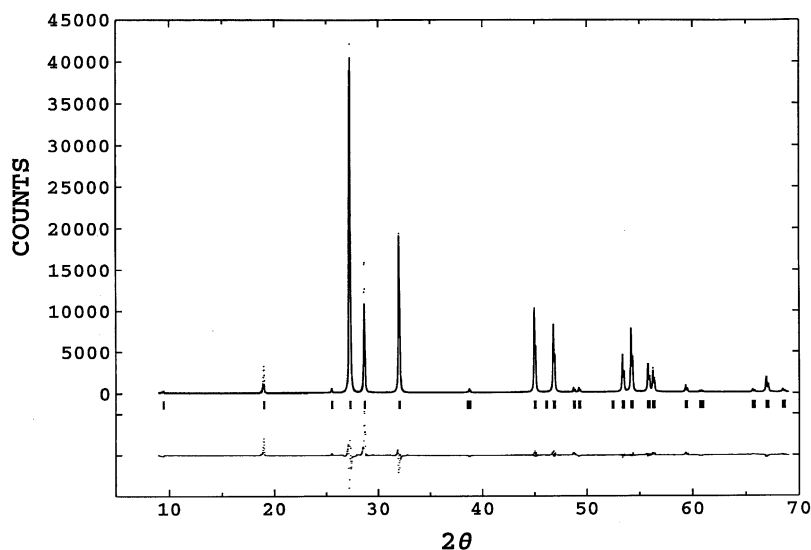


Fig. 4. Observed, calculated and difference profiles for $\text{Bi}_{3.24}\text{La}_2\text{W}_{0.76}\text{O}_{10.14}$.

Table 3

Estimated atomic coordinates, occupancy factors (OF), and isotropic thermal parameters (B_{iso}) of $\text{Bi}_{3.24}\text{La}_2\text{W}_{0.76}\text{O}_{10.14}$

Atom	Site	OF	x	y	z	B_{iso} (\AA^2)
La	2a	1	0.0	0.0	0.0	0.65
$\text{Bi}_{3.24}\text{W}_{0.76}$	4i	1	0.330	0.0	0.320	2.30
O(1)	4i	0.845	0.333	0.0	0.083	0.30
O(2)	4i	0.845	0.166	0.0	0.416	0.30
O(3)	4i	0.845	0.0	0.0	0.25	0.30

Fig. 5 represents DTA results of the three $\text{Bi}_{3.24}\text{Ln}_2\text{W}_{0.76}\text{O}_{10.14}$ compounds. All samples showed two polymorphic phase transitions which are reversible with remarkable thermal hysteresis. On heating, a weak and somewhat broad peak occurs at about 980°C in common but another sharp endothermic peak appears at temperatures of 1097 – 1210°C depending on Ln. In the light of the supercell–subcell relationship mentioned above, two phase transitions may be connected with the structural changes. That is, on heating, the monoclinic (nearly orthorhombic) starting phase transforms probably to the hexagonal (rhombohedral) phase around 980°C , and the hexagonal phase may revert to the fcc phase through the higher transition temperature. The examination of the actual structural changes by high-temperature X-ray diffraction will be the subject of future study.

Fig. 6 exhibits the variation of electrical conductivity, $\log(\sigma)$, with temperature for the three $\text{Bi}_{3.24}\text{Ln}_2\text{W}_{0.76}\text{O}_{10.14}$ compounds. As discussed above, since the structure of these compounds is based on an oxygen-deficient pseudo-fcc subcell which is probably related to that of $\delta\text{-Bi}_2\text{O}_3$ which is the high-temperature stable modification and shows an excellent oxide-ion

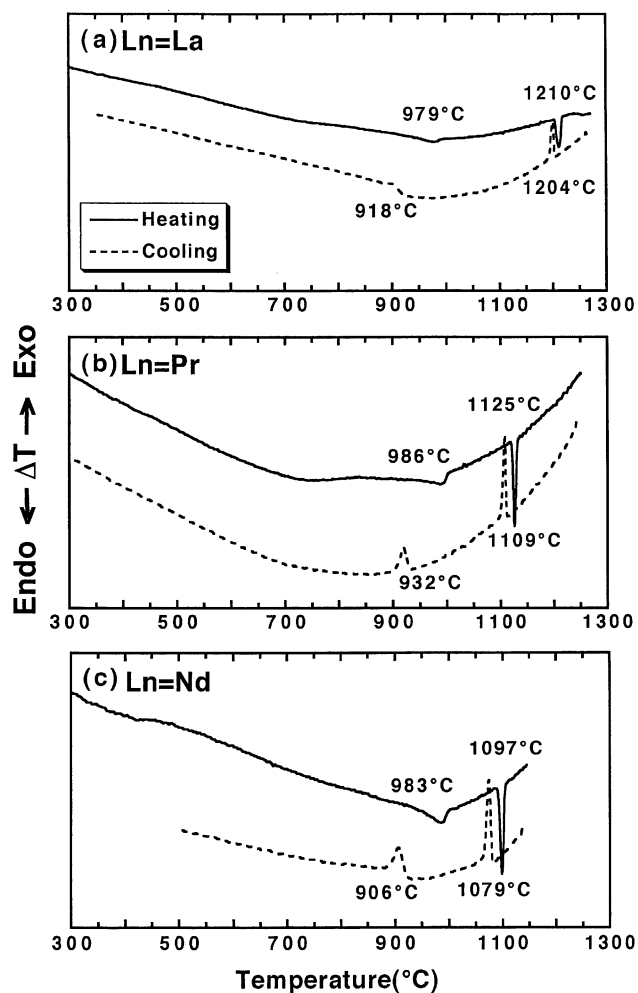


Fig. 5. DTA curves in the heating and cooling cycle for $\text{Bi}_{3.24}\text{Ln}_2\text{W}_{0.76}\text{O}_{10.14}$ at a rate of $10^\circ\text{C min}^{-1}$ and (a) $\text{Ln} = \text{La}$, (b) $\text{Ln} = \text{Pr}$, and (c) $\text{Ln} = \text{Nd}$. The solid lines are heating process and the broken lines cooling process.

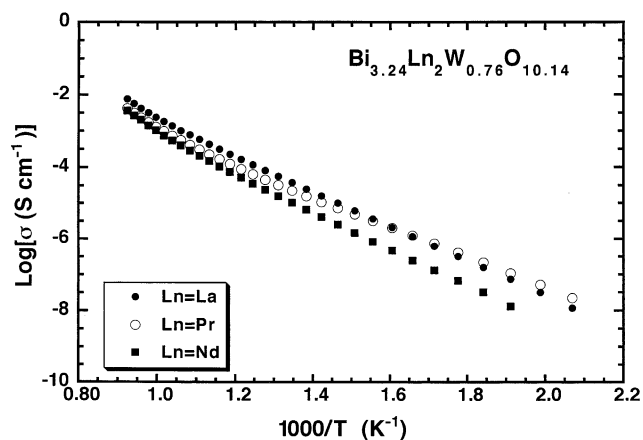


Fig. 6. Arrhenius plots of electrical conductivity σ (S cm^{-1}) of $\text{Bi}_{3.24}\text{Ln}_2\text{W}_{0.76}\text{O}_{10.14}$.

conduction [15], they are expected to exhibit a high conductivity even in a lower temperature region. In contrast, the results yield useless conductivity values as shown. In all probability, the oxygen atoms in the monoclinic structure must be ordered so that the oxygen atoms cannot move easily.

4. Conclusion

The new compounds $\text{Bi}_{3.24}\text{Ln}_2\text{W}_{0.76}\text{O}_{10.14}$ have been obtained only in $\text{Ln} = \text{La}$, Pr , and Nd . Although the crystal lattice of the new compound could be regarded as orthohexagonal, its true symmetry turned out to be monoclinic with $\beta \approx 90^\circ$ by taking account of the cation configuration which can easily be estimated using a supercell–subcell relationship. That is, the monoclinic cell forms a superstructure based on a pseudo-fcc subcell

($a' \approx 5.6 \text{ \AA}$) which is thought of as related to $\delta\text{-Bi}_2\text{O}_3$. All the new compounds, however, exhibit lower conductivities far from an application.

Acknowledgments

This work was supported by CREST of Japan Science and Technology, and the author thanks Drs. M. Onoda and K. Das for the Rietveld analysis and Dr. M. Nespola for helpful discussions.

References

- [1] A. Watanabe, Z. Inoue, T. Ohsaka, *Mater. Res. Bull.* 15 (1980) 397.
- [2] A. Watanabe, *Mater. Res. Bull.* 15 (1980) 1473.
- [3] R.W. Wolfe, R.E. Newnham, M.I. Kay, *Solid State Commun.* 7 (1969) 1797.
- [4] E.C. Subbarao, *J. Phys. Chem. Solids* 23 (1962) 665.
- [5] L.E. Cross, *Ferroelectricity and Conduction in Ferroelectric Crystals*, Tech. Rep. AFAL-TR-72-146, 1972.
- [6] A. Watanabe, Y. Sekikawa, F. Izumi, *J. Solid State Chem.* 41 (1982) 138.
- [7] A. Watanabe, *Mater. Res. Bull.* 19 (1984) 877.
- [8] J.W. Visser, *J. Appl. Crystallogr.* 2 (1969) 89.
- [9] D.E. Appleman, H.T. Evans Jr., NTIS PB-216 (1973) 188.
- [10] F. Izumi, in: R.A. Young (Ed.), *The Rietveld Method*, Oxford University Press, Oxford, 1993, p. 236 (Chapter 13).
- [11] R.D. Shannon, *Acta Crystallogr. A* 32 (1976) 751.
- [12] H.A. Harwig, *Z. Anorg. Allg. Chem.* 444 (1978) 151.
- [13] H. Arnold, in: T. Hahn (Ed.), *International Tables for Crystallography*, Vol. A, D. Reidel Publishing Company, Dordrecht, 1983, p. 79 (Chapter 5).
- [14] T. Hahn (Ed.), *International Tables for Crystallography*, Vol. A, D. Reidel Publishing Company, Dordrecht, 1983, pp. 158–160 (Chapter 7).
- [15] H.A. Harwig, A.G. Gerards, *J. Solid State Chem.* 26 (1978) 265.